ACS OMEGA

Article

Cite This: ACS Omega XXXX, XXX, XXX−XXX

http://pubs.acs.org/journal/acsodf

Magnetically Actuated Tunable Soft Electronics

Mahdi Ilami,[†] Reza J. Ahmed,[†] Dakota Edwards,[†] Erskine Thompson,[†] Saeed Zeinolabedinzadeh,[‡] and Hamidreza Marvi*[,†]

[†]School for Engineering of Matter, Transport and Energy and [‡]School of Electrical, Computer and Energy Engineering, The Arizona State University, Tempe, Arizona 85281, United States

Supporting Information

ABSTRACT: Variable electronics are vital in tunable filters, transmitters, and receivers, among other applications. In addition, the ability to remotely tune soft capacitors, resistors, and inductors is important for applications in which the device is not accessible. In this paper, a uniform method of remotely tuning the characteristic properties of soft electronic units (i.e. inductance, capacitance, and resistance) is presented. In this method, magnetically actuated ferrofluid mixed with iron powder is dragged in a soft fluidic channel made of polydimethylsiloxane (PDMS) to tune the electrical properties of the component. The effects of position and quantity of the ferrofluid and iron powder are studied over a range of frequencies, and the changes in inductance, capacitance, resistance, quality factor, and self-resonance frequency are reported accordingly. The position plays a bigger role in changing inductance, capacitance, and resistance. With the proposed design, the inductance can be changed by 20.9% from 3.31 μH for planar inductors and 23% from 0.44 μH for axial inductors. In addition, the capacitance of capacitors and impedance of resistors can be changed by 12.7% from 2.854 pF and 185.3% from 0.353 kΩ, respectively. Furthermore, the changes in the inductance, capacitance, and resistance follow "quasi-linear profiles" with the input during position and quantity effect experiments.

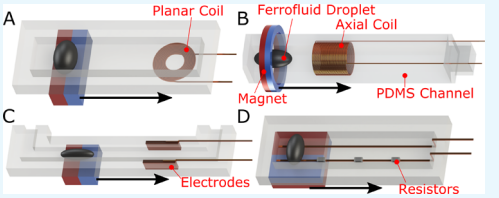

1. INTRODUCTION

Soft electronics is considered to be a promising replacement for traditional rigid circuits in specialized applications where flexibility, stretchability, and biocompatibility are required. Current commercial integration of soft electronics is limited, but the true measure of this technology's value lies in its potential. Improvements in soft electronics will open doors in several fields. Soft robotics will achieve mobility in highly confined spaces, passively distributing stress to attain robots more robust to their environments.[1−4]

In particular, variable electronic components are vital to applications requiring any type of tuning. Variable resistors are extensively used as control inputs to electronic circuits. Variable inductors can be used for voltage regulation, in tuning the frequencies of inductively coupled power transfer systems and power factor correction over long distances.[5−7] Variable capacitors can also be used for tuning the resonance frequency and capacitive reactance of electrical circuits.[8] In addition, variable components serve a vital purpose in tunable filters, receivers, and transmitters.[9,10] The addition of these functions will significantly enhance the toolbox of soft electronic device designers.

Through the pursuit of these functionalities, a variety of methods have been developed for achieving soft electronic components and devices. These methods fall into three categories: material innovation, structural design,[11] and mobile liquid conductors. Through material innovation,[12,13] researchers produced conductive composite materials by depositing/embedding conductive nanomaterials onto/within a stretchable substrate.[14] The resulting composite material is characterized by the conductive properties of the nanomaterial and the mechanical properties of the substrate. Moreover, by using intrinsically stretchable materials such as polydimethylsiloxane (PDMS) doped with nickel, silver, or R-GO microtubes, stretchable electronic devices can be developed.[15] These intrinsically stretchable conductive materials can be produced at a low cost because of their simple fabrication process and are characterized by high integrity when stacked in layers. In the structural design category,[16−18] stretchable interconnects such as waves,[19,20] bridges,[21] or meanders of a rigid conductor,[22] conductor-filled polymers,[23] or microfluidic filled with static liquid metals are used to achieve high electrical conductance when bonded to or used in conjunction with stretchable substrates. These stretchable substrates are usually composed of either an elastomeric membrane,[24] a net made of elastomer,[25] or a stretched and flattened flex circuit polymer foil.[26] For instance, Gray et al. constructed elastomeric electronics by embedding a common helical spring in an elastomer using lithography techniques.[27] In addition, using out of plane wavy geometries of solid conductor strands embedded onto a prestrained elastomer substrate, Choi et al. produced stretchable conductive composites. The effectiveness of this method depends largely on the design of the waves and meander patterns of the solid conductor.[19]

Besides the abovementioned methods, liquid conductors have also been used to develop soft electronic components and

Received: August 22, 2019
Accepted: November 19, 2019

DOI: 10.1021/acsomega.9b02716
ACS Omega XXXX, XXX, XXX−XXX

Table 1. Minimum and Maximum Inductance, Q-Factor, and SRF of Planar Inductors for Different Positions and Quantities of the Mobile Components[a]

case	min(L) ± SEM	max(L) ± SEM	min(Q) ± SEM	max(Q) ± SEM	min(SRF) ± SEM	max(SRF) ± SEM
(1)	4.092 ± 0.069	4.154 ± 0.079	21.7 ± 0.4	23.5 ± 0.6	32.8 ± 1.9	33.0 ± 2.0
(2)	3.320 ± 0.118	3.347 ± 0.117	20.2 ± 1.2	21.4 ± 1.1	36.2 ± 2.3	36.3 ± 2.4
(3)	2.994 ± 0.303	3.081 ± 0.208	16.6 ± 2.2	17.9 ± 1.2	37.0 ± 0.8	37.3 ± 0.6
(4)	3.319 ± 0.069	3.330 ± 0.103	21.6 ± 0.9	22.0 ± 1.4	36.2 ± 2.3	37.5 ± 0.3
(5)	4.025 ± 0.070	4.081 ± 0.058	23.1 ± 0.6	25.1 ± 1.3	32.9 ± 2.0	33.4 ± 2.2
(6)	3.280 ± 0.047	3.753 ± 0.196	18.4 ± 0.4	23.5 ± 2.9	34.3 ± 1.4	35.7 ± 2.0
(7)[b]	**3.309 ± 0.034**	**4.000 ± 0.056**	**19.1 ± 0.7**	**26.6 ± 0.7**	**33.5 ± 2.1**	**35.5 ± 2.3**
(8)	3.327 ± 0.066	3.953 ± 0.026	21.9 ± 1.3	27.1 ± 1.1	34.2 ± 2.1	37.4 ± 0.3
(9)	3.318 ± 0.120	3.990 ± 0.052	21.9 ± 1.2	26.7 ± 0.9	33.7 ± 2.0	36.2 ± 2.3

[a]The inductances are measured at a frequency of 10 MHz and Q-factors at the peak. Minimum, maximum, and the standard error of the mean are calculated based on the data collected from three planar inductors with the same design. The inductances are in μH and the self-resonance frequencies are in MHz. Cases studied in quantity-effect experiments include changing the mass of iron without the magnet being present (case (1)), changing the mass of iron with the magnet being present (case (2)), changing the mass of iron with the magnet and ferrofluid being present (case (3)), and changing the volume of ferrofluid with the magnet being present (case (4)). Cases studied in position-effect experiments include moving iron without the magnet being present (case (5)), iron with the magnet being present (case (6)), a mixture of iron and ferrofluid with the magnet being present (case (7)), ferrofluid with the magnet being present (case (8)), and only the magnet (case (9)). [b]Case (7) offers the broadest tuning range for inductance among the planar inductors evaluated in this study.

devices.[28,29] In this category, development of soft electronics is aided by existing research, concepts, and inventions in the field of microfluidics. Microfluidics is the science of manipulating fluids at the micrometer scale; when a conductive fluid is used, it represents a very viable approach to creating soft, stretchable electronics at a similarly small scale.

The emergence of microfluidics in soft electronics opened a new era, toward using fluids such as liquid metals in electronics. Microfluidic-based electronics is a combination of well-established fields and has evolved largely in the last two decades. Researchers demonstrated that in addition to microfluidic electronic components made of static liquid metal, mobile liquid metals can also be utilized in such components. Jeon et al. used liquid metals with magnetic manipulation to make electrical switches.[30] In another study, Wang et al. developed a reconfigurable liquid metal antenna driven by electrochemically controlled capillarity.[31]

In addition to liquid metals, ferrofluids are also used for microfluidic electronic applications. Ferrofluid is made of ferromagnetic particles suspended in a carrier fluid. The carrier fluid can be a water or an organic solvent, and ferromagnetic particles are covered with a surfactant to prevent them from clumping.[32] The carrier fluid and surfactant can both be chosen from biocompatible materials, as in commercially available biocompatible ferrofluids. Micro-magnetofluidics is a subfield in microfluidics which studies the use of ferrofluid and other types of magnetic fluids in microfluidic environments. Micro-magnetofluidics has been successfully used for flow control,[33] particle sorting and separation,[34] pumps and valves,[35] micromixing and assaying,[36] and droplet formation.[37] Although ferrofluids alone are nonconductive, conductive liquid metal-based ferrofluids have been produced.[38−41]

Currently, a few tunable microfluidic soft electronic components have been designed and developed. Lazarus et al. devised a stretchable, variable inductor with gallium-filled microfluidic channels in a silicone elastomer and with a ferrofluid core and successfully tested it to 100% strain.[42] Assadsangabi invented a variable planar inductor using ferrofluid as a core and achieved variability by manipulating the ferrofluid.[43] In their design, a second planar coil and a permanent magnet lie beneath the inductor in order to manipulate the ferrofluid in a chamber above the inductor. Polcar and Mayer devised a magnetically controllable variable capacitor which uses ferrofluid as the dielectric medium.[44] Using a magnetic field to manipulate the ferrofluid dielectric between plates, a variable capacitance is achieved. Furthermore, Liu et al. introduced a variable capacitor made of two stretchable channels filled with liquid metals.[45] Although many of the previously developed microfluidic electronic components are classified as stretchable, flexible, bendable, and/or variable, no research to date presents a full trio of variable electrical components that are tuned via a standardized method. Current variable soft electrical components are variable but most of them require power to be continuously applied in order to maintain a specific characteristic value. Furthermore, many of these soft variable electronics must be directly adjusted instead of being adjusted remotely.

In this paper, microfluidic soft variable resistors, capacitors, and inductors are presented, all with a standardized tuning method. This method enables remote, magnetic tuning that does not expend power to maintain a tuned characteristic value. The proposed method for tuning the characteristics of the electrical components is based on the effect of a mobile component, which travels through a soft channel. By choosing the mobile component from magnetically responsive materials, it can be actuated using a magnetic field remotely. Having this in mind, ferrofluid is chosen as the mobile component of the proposed stretchable variable electronic units. Additionally, using iron particles as well as mixture of iron particles and ferrofluid is explored as alternatives. This study, explores the effects of volume of ferrofluid, mass of iron, and different ratios of their mixture, in different positions inside the channel with and without a magnet on the characteristics of each electronic unit. In particular, a vector network analyzer (VNA) is used to measure the effect of the mobile component on inductance, quality-factor (Q-factor), and self-resonance frequency (SRF) of the inductors, capacitance, Q-factor, and SRF of capacitors, and impedance of the resistors.

2. RESULTS AND DISCUSSION

In this section, the effect of quantity (cases 1−4; as described in section 4.2.1) and position (cases 5−9; as described in section 4.2.2) of the mobile components on inductance, Q-

DOI: 10.1021/acsomega.9b02716
ACS Omega XXXX, XXX, XXX−XXX

Table 2. Minimum and Maximum Inductance, *Q*-Factor, and SRF of Axial Inductors for Different Positions and Quantities of the Mobile Components[a]

case	min(L) ± SEM	max(L) ± SEM	min(Q) ± SEM	max(Q) ± SEM	min(SRF) ± SEM	max(SRF) ± SEM
(1)	0.653 ± 0.007	0.695 ± 0.039	8.4 ± 0.4	9.8 ± 1.0	103.5 ± 4.3	105.5 ± 1.9
(2)	0.427 ± 0.016	0.457 ± 0.009	21.6 ± 5.2	43.1 ± 9.9	122.4 ± 2.5	125.8 ± 2.5
(3)	0.422 ± 0.020	0.438 ± 0.022	27.3 ± 2.0	52.2 ± 11.8	123.5 ± 3.5	125.7 ± 3.9
(4)	0.419 ± 0.018	0.487 ± 0.061	50.3 ± 1.4	58.9 ± 14.9	111.1 ± 4.4	120.5 ± 8.2
(5)	0.517 ± 0.045	0.526 ± 0.049	29.6 ± 8.1	35.1 ± 11.3	115.3 ± 1.7	116.0 ± 1.5
(6)	0.457 ± 0.009	0.510 ± 0.016	21.6 ± 5.2	42.1 ± 8.1	116.6 ± 3.2	122.4 ± 2.5
(7)[b]	**0.438 ± 0.022**	**0.538 ± 0.023**	**27.3 ± 2.0**	**59.8 ± 24.9**	**112.9 ± 0.7**	**123.5 ± 3.5**
(8)	0.443 ± 0.037	0.467 ± 0.028	59.8 ± 13.1	79.3 ± 12.9	114.6 ± 6.4	118.2 ± 10.6
(9)	0.417 ± 0.016	0.490 ± 0.028	58.8 ± 15.3	75.3 ± 6.8	113.1 ± 9.1	121.4 ± 9.6

[a]The inductances are measured at a frequency of 10 MHz and *Q*-factors at the peak. Minimum, maximum, and the standard error of the mean are calculated based on the data collected from three different axial inductors of cross section 3 mm × 3 mm with the same design. The inductances are in μH and the self-resonance frequencies are in MHz. Cases studied in quantity-effect experiments include changing the mass of iron without the magnet being present (case (1)), changing the mass of iron with the magnet being present (case (2)), changing the mass of iron with the magnet and ferrofluid being present (case (3)), and changing the volume of ferrofluid with the magnet being present (case (4)). Cases studied in position-effect experiments include moving iron without the magnet being present (case (5)), iron with the magnet being present (case (6)), a mixture of iron and ferrofluid with the magnet being present (case (7)), ferrofluid with the magnet being present (case (8)), and only the magnet (case (9)). [b]Case (7) offers the broadest tuning range for inductance among the axial inductors evaluated in this study.

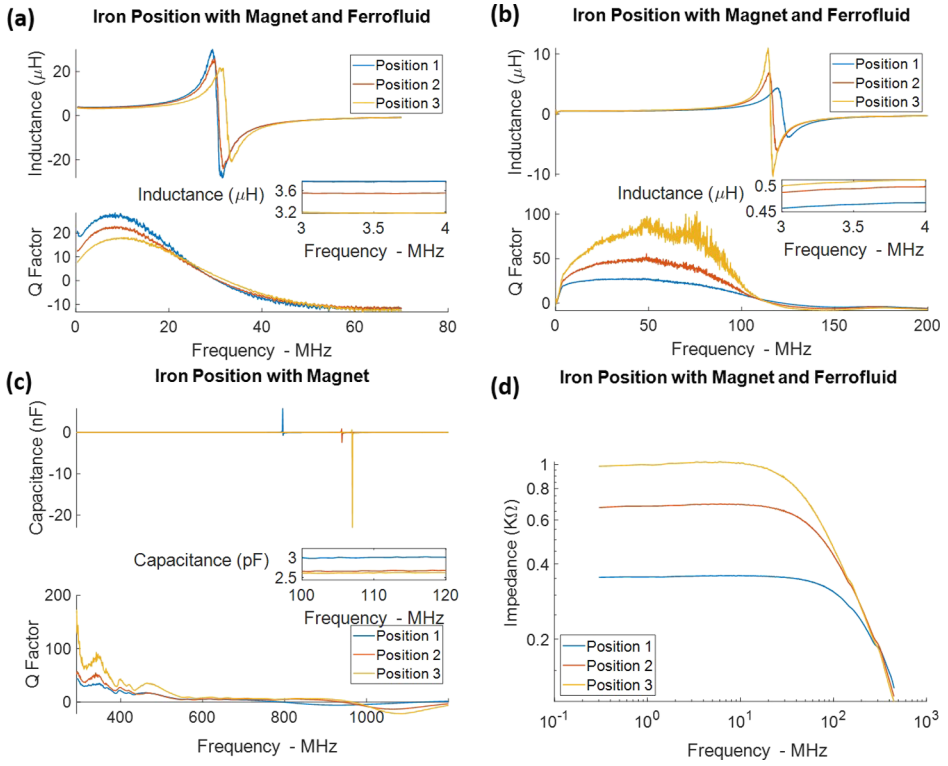

Figure 1. Experiments with the most significant change in the tuning range for (a) planar inductor, (b) axial inductor, (c) capacitor, and (d) resistor.

factor, and SRF of the inductors; capacitance, *Q*-factor, and SRF of capacitors; and impedance of the resistors are discussed in detail.

2.1. Inductors. Tables 1 and 2 illustrate the results of both position-effect and quantity-effect experiments with the planar and axial inductors, respectively. Among planar inductors, as can be seen in Table 1, case (3) among the quantity-effect and case (7) among the position-effect experiments achieved the broadest tuning range for inductance [2.9% for case (3) and 20.9% for case (7)]. In this table, the inductance is measured at a frequency of 10 MHz.

For the axial inductors, case (4) among the quantity-effect and case (7) among the position-effect experiments are the most successful in increasing inductance [increase of 16.33% for case (4) and 23% for case (7)]. From the figures and measurements, it can be concluded that for all of the planar and axial inductors explored in this study, moving the mobile component results in more significant changes in inductance than changing its quantity. In Table 2, the inductance is measured at a frequency of 1.5 MHz and the *Q*-factor at the peak.

The spectral magnitude and spectral phase of the inductors are illustrated in the Supporting Information. As is clear in

DOI: 10.1021/acsomega.9b02716
ACS Omega XXXX, XXX, XXX−XXX

Table 3. Minimum and Maximum Capacitance, *Q*-Factor, and SRF of the Capacitors for Different Positions and Quantities of the Mobile Components[a]

case	min(C) ± SEM	max(C) ± SEM	min(Q) ± SEM	max(Q) ± SEM	min(SRF) ± SEM	max(SRF) ± SEM
(1)	2.882 ± 0.138	2.977 ± 0.169	16.3 ± 3.5	19.6 ± 1.7	877.6 ± 21.1	915.5 ± 15.6
(2)	3.086 ± 0.064	3.108 ± 0.011	15.0 ± 0.2	17.6 ± 1.3	854.0 ± 44.3	864.6 ± 37.0
(3)	3.035 ± 0.255	3.082 ± 0.180	24.7 ± 6.5	26.8 ± 7.6	863.8 ± 21.2	888.4 ± 43.5
(4)	2.947 ± 0.195	2.977 ± 0.217	16.1 ± 1.6	20.6 ± 9.1	906.3 ± 33.8	920.4 ± 27.0
(5)	2.797 ± 0.134	2.977 ± 0.169	14.3 ± 2.5	19.6 ± 1.7	877.6 ± 21.1	959.9 ± 12.1
(6)[b]	**2.854 ± 0.174**	**3.218 ± 0.086**	**15.5 ± 1.8**	**23.2 ± 7.7**	**814.8 ± 13.6**	**946.4 ± 26.2**
(7)	2.855 ± 0.201	3.059 ± 0.162	17.9 ± 5.7	21.7 ± 3.8	876.0 ± 17.1	951.5 ± 29.0
(8)	2.950 ± 0.288	2.981 ± 0.213	15.4 ± 4.1	23.6 ± 10.4	904.4 ± 31.2	920.4 ± 57.5
(9)	2.802 ± 0.113	2.930 ± 0.190	13.4 ± 1.5	18.3 ± 4.9	921.2 ± 25.4	955.0 ± 12.0

[a]The capacitances and *Q*-factors are measured at a frequency of 243 MHz. Minimum, maximum, and the standard error of the mean are calculated based on the data collected from three different capacitors with the same design. The capacitances are in pF and the self-resonance frequencies are in MHz. Cases studied in quantity-effect experiments include changing the mass of iron without the magnet being present (case (1)), changing the mass of iron with the magnet being present (case (2)), changing the mass of iron with the magnet and ferrofluid being present (case (3)), and changing the volume of ferrofluid with the magnet being present (case (4)). Cases studied in position-effect experiments include moving iron without the magnet being present (case (5)), iron with the magnet being present (case (6)), a mixture of iron and ferrofluid with the magnet being present (case (7)), ferrofluid with the magnet being present (case (8)), and only the magnet (case (9)). [b]Case (6) offers the broadest tuning range for capacitance among the capacitors evaluated in this study.

each phase plot, the phase switches sign at the SRF. The nonlinear behavior of magnitude at frequencies approaching zero is due to a limit of the VNA.

The changes in characteristics of the planar and axial inductors under the position and quantity effects are due to the relation of inductance and the magnetic permeability of the material in proximity to the inductor. The increase in permeability is due to the introduction and incremental addition of iron particles and ferrofluid (ferromagnetic materials) to the inductor, both having relative permeability greater than one. In cases (1−4), different concentrations of iron particles and ferrofluid are used. By increasing the amount of iron particles or ferrofluid, the effect on the inductance is increased. In cases (5−8), moving the mobile component to the core of the inductors causes the maximum effect. The differences in the level of effectiveness between cases using iron particles [case (1−3) and (5−7)] and cases using ferrofluid [cases (4) and (8)] are due to the lower concentration of ferrite particles in the ferrofluid. In case (9), bringing the magnet close to the inductor disrupts its magnetic field lines and changes the permeability of space proximal to the inductor, which alters the unit's inductance.

The *Q*-factor relates the stored energy in the inductor to the dissipated energy, which is typically defined as the ratio of the reactance value to the equivalent resistance value at a given frequency, using a narrow-band approximation approach. The maximum observed change in *Q*-factor of planar inductors is 8.5% in quantity-effect experiments [case (2)] and 39% in position-effect experiments [case (7)]. In Table 1, the *Q*-factor is measured at its peak point. Inductance and *Q*-factor of case (7) are plotted over the frequency range of 0.3−70 MHz in Figure 1a. The effect of position and quantity of the mobile components on three planar inductors is plotted in Figures S3−S5 in the Supporting Information.

Regarding *Q*-factor of axial inductors (Table 2), of quantity-effect experiments, the maximum change is 99% in case (2) and of position-effect experiments, the maximum change is 119% in case (7). Inductance and *Q*-factor of case (7) are plotted over the frequency range of 0.3−200 MHz in Figure 1b. In addition, the effect of position and quantity of the mobile component on three axial inductors is plotted in Figures S6−S8 in the Supporting Information.

It is known that an increase in the inductance results in an increase in stored energy, and thus an increase in *Q*-factor is expected. Over all experiments, the changes in inductance are greater in cases (5−9); *Q*-factor similarly experiences larger changes in these cases, as compared to cases (1−4). However, *Q*-factor does not linearly change with respect to inductance. Additionally, the presence of a ferrite core can increase the loss and decrease the *Q*-factor to some extent. As a result of these competing factors, the net change observed in the *Q*-factor is moderate.

SRF is also affected by changing either the position or quantity of the mobile components. For planar inductors (Table 1), the quantity of the mobile component has a minimal impact on SRF (less than 4%), while its position change results in shifting the SRF more significantly [7.3% for case (9) and 9.4% for case (8)]. For axial inductors (Table 2), case (4) induced the greatest shift in SRF among quantity-effect experiments (8.46%) and among position-effect experiments, case (7) shifts the SRF more significantly (9.36%). SRF of an inductor is inversely proportional to the value of the inductance; therefore a decrease in SRF is expected from an increase in the inductance value of the component.

2.2. Capacitors. The results of both position-effect and quantity-effect experiments for capacitors are detailed in Table 3. In this table, both the capacitance and *Q*-factor are measured at a frequency of 243 MHz. Results of the experiments conducted on capacitors are plotted in Figures S9−S11 in the Supporting Information. In addition, the spectral magnitude and spectral phase of the capacitors are also plotted in the Supporting Information.

In resemblance to the inductor experiments, it is found that for the capacitors explored in this study, moving the mobile component results in more significant tunability of capacitance than changing its quantity. Of the position-effect experiments, case (6) produces the greatest tuning range of capacitance (increase of 12.7%), and of the quantity-effect experiments, case (2) is the most effective scenario for tuning of capacitance (increase of 6.5%). Capacitance and *Q*-factor of case (6) are plotted over the frequency range of 0.3−1200 MHz in Figure 1c.

In cases (1−3) and (5−7), iron particles conglomerate inside the channels near the magnet resulting in a conductive

DOI: 10.1021/acsomega.9b02716
ACS Omega XXXX, XXX, XXX−XXX

clustered medium. Considering the thin layer of PDMS between the clustered iron particle medium and each plate, this electronic unit can be conceptualized as two capacitors in series. The total capacitance decreases as the conductive medium grows larger in area. This increase in area is facilitated by either changing the amount of iron particles between the capacitor electrodes through adding more iron particles [cases (1−3)] or moving the mobile component further toward the center of the capacitor's plates [cases (5−7)]. This effect is more significant in the presence of the magnet in cases (2) and (6), as the iron particles under the influence of the magnetic field are more closely forced together between the capacitor plates. This increases the amount of mobile component material between the plates, leaving fewer and smaller air gaps in the conductive cluster in comparison to cases (1) and (5). In cases (3) and (7), using ferrofluid along with iron particles shows counter effects or only moderate changes: the variations in capacitance are smaller in these cases compared to cases (2) and (6), in which ferrofluid is not used. Small effects on capacitance seen in cases (4) and (8) are due to the small dielectric permittivity of ferrofluid which is close to that of air.

Maximum *Q*-factor change in quantity-effect studies is 36.6% in case (2). Of position-effect experiments, maximum *Q*-factor change is 53% in case (8). For capacitors, the changes in *Q*-factor are due to changes in the ratio of stored to dissipated energy. This relation is formulated in eq 5 showing that through an increase in the capacitance, the *Q*-factor decreases. In cases (5−7), moving the iron particles between the plates results in a decrease in the capacitance and thus, an increase in the *Q*-factor. This relation is not linear, as iron particles introduce conduction losses which decrease the *Q*-factor. In cases (3−4 and 7−8), ferrofluid acts as a dielectric and introduces dielectric loss. Therefore, the net change in the *Q*-factor is subdued.

With regards to the SRF of capacitors, the results indicate that the change in the amount of the mobile component has only a slight effect on the SRF (less than 9%) while the position of the mobile component causes a more significant shift in the SRF (up to 16%) (Figure S9 in the Supporting Information). SRF of capacitors is inversely proportional to the value of the capacitance. Because the capacitance experiences bigger changes during position-effect experiments, SRF will undergo a more significant shift in these experiments as well.

2.3. Resistors. Figure S12a in the Supporting Information shows that the circuit is open when using the mobile component comprised of iron powder without a magnet, as the resistance is too high regardless of the iron mass. Likewise, Figure S12b illustrates that the ferrofluid used in these experiments is not electrically conductive. These results reduce the number of possible experiments which may have an impact on the impedance to four different cases: changing the mass of iron with the magnet being present (case (1)), changing the volume of ferrofluid mixed with iron particles and magnet being present (case (2)), changing the position of iron particles with the magnet (case (3)), and changing the position of iron particles mixed with ferrofluid using a magnet (case (4)). The results of these experiments are shown in Figures S12c−f, S13, and S14 in the Supporting Information over the frequency range of 0.3−450 MHz.

Figure S12c illustrates that by adding more iron powder under the influence of the magnet (case (1)), the resistance of the mobile component drops. This is due to the alignment of iron particles along the magnetic field direction of two magnets with the configuration shown in Figure 3c, which bridges two wires and connects the circuit. By increasing the amount of iron, the surface area of the mobile component connecting the two wires increases, which leads to a better conductivity. Figure S12d (case (2)) in the Supporting Information shows a slight improvement in the conductivity of the mobile component on adding ferrofluid to it. Adding ferrofluid to iron particles enhances the particles alignment which is likely the reason of slight improvement in conductivity of the mobile component in case (2). Figure S12e (case (3)) illustrates the change in the impedance by moving the mobile component in different positions. This is due to different numbers of resistors being included in the circuit. Finally, Figure S12f (case (4)) shows that adding ferrofluid to the mobile component can improve the result of the position experiment slightly.

Table 4 contains the results of both position-effect and quantity-effect experiments for resistors. The impedance of the resistors is measured at 692 kHz. According to the data, the iron amount (case (1)) has more influence on the conductivity of the mobile component than ferrofluid volume (case (2)). Furthermore, in the position-effect experiments, the resistance of mobile component in case (4) is less than case (3).

Table 4. Minimum and Maximum Impedance for Different Position and Quantity Cases for Resistors[a]

case	min ± SEM	max ± SEM
(1)	0.359 ± 0.007	0.425 ± 0.028
(2)	0.353 ± 0.004	0.354 ± 0.005
(3)	0.359 ± 0.007	1.026 ± 0.006
(4)[b]	**0.353 ± 0.004**	**1.012 ± 0.003**

[a]The impedances are measured at a frequency of 692 kHz. Minimum, maximum, and the standard error of the mean are calculated based on the data collected from three different resistors. The impedances are in kΩ. Cases studied in quantity-effect experiments include changing the mass of iron with the magnet being present (case (1)) and changing the volume of ferrofluid mixed with iron particles and magnet being present (case (2)). Cases studied in position-effect experiments include changing the position of iron particles with the magnet (case (3)) and changing the position of iron particles mixed with ferrofluid using a magnet (case (4)). [b]Case (4) offers the broadest tuning range for impedance among the resistors evaluated in this study.

3. CONCLUSION

In this paper, we propose a uniform method to add tunability to soft electronic units including inductors, capacitors, and resistors. This method changes the characteristics of soft electronic units using a mobile component moving in a fluidic channel. The effects of both position and quantity of the mobile components on electrical characteristics of each circuit element were fully explored. The results show that the position of the mobile component has more impact on changing the characteristics of the electronic unit. In particular, we show that the inductance of planar inductors can change up to 20.9% from 3.31 μH by using a mixture of iron and ferrofluid as the mobile component with the magnet being present, the inductance of axial inductors up to 23% from 0.44 μH by utilizing a mixture of iron and ferrofluid as the mobile component with the magnet being present, the capacitance of capacitors up to 12.7% from 2.854 pF under the influence of iron particles as the mobile component with the magnet being present, and impedance of resistors up to 185.3% from 0.353

DOI: 10.1021/acsomega.9b02716
ACS Omega XXXX, XXX, XXX−XXX

kΩ by moving the mobile component made of iron particles. In addition, it is shown that the Q-factor of planar inductors changes up to 39% from 19.1, axial inductors up to 119% from 27.3, and capacitors up to 53% from 15.5. The changes in the inductance, capacitance, and resistance follow "quasi-linear profiles" with the input during position and quantity effect experiments. This means that the mobile component can be encapsulated inside the channel and actuated remotely to tune the characteristics of an electronic unit. Moreover, the possibility of using different mixing ratios of iron particles and ferrofluid can provide different tuning ranges and thus different tuning resolutions for the same displacement of the mobile component. This technique can be used for developing tunable electronics with wide tuning ranges (e.g. filters, receivers, and transmitters) for a variety of applications.

4. METHODS

This study is conducted on resistors, capacitors, and two types of inductors (i.e. one planar inductor and one axial inductor). Three samples of each type are fabricated for data collection. In this section, fabrication processes, experiments, measurements, and calculations are discussed.

4.1. Electronic Units Fabrication. All of the units proposed in this study have three main components: a fluidic channel, an electrical component, and a mobile component. Fabrication of each of these components is described in details in the following.

4.1.1. Fluidic Channel. Fluidic channels are designed to contain the mobile component and provide it with a path to move through. These channels are made of PDMS and are fabricated using soft lithography.[46] The PDMS used for channel fabrication is Dow and Corning's Sylgard 184, with the mixing ratio of 1:10.

3D printing is used to fabricate the negative channel patterns. After printing the molds, silicone oil is applied to the surface for ease of demolding. The oil is left on the surface for 1 min, then the excess is lightly blown off, and the mold is put on the hot plate at 90 °C for 10 min. After mixing, the air bubbles trapped in PDMS are released using a vacuum chamber (degassing), and then it is poured into the molds and degassed again. Finally, the molds are placed on a hot plate set to 90 °C for 3 h. Planar coils and resistors (Figure 2a,d) have the same design of channels; first, the channel walls are fabricated out of PDMS. Then, these walls are mounted on a glass slide to complete the channel. Although this can similarly be done by using a layer of PDMS instead of a glass slide, the focus of this study is not on the effect of stretching or twisting the channel. Therefore, glass slides are chosen to eliminate any coupled effects due to unwanted deformation of the channels during the experiments. These channels are 70 mm long, 15 mm wide, and 10 mm deep with the wall thickness of 7 mm on the sides and 4 mm at both ends.

Axial inductors (Figure 2b) are made in two steps: in the first step, a thin wall channel with 0.5 mm thickness is fabricated and copper wire is wound around it; a 3D printed cubic core is placed inside the channel to reinforce the thin layered PDMS and prevent any deformations during wire winding. In the second step, the channel and the coil go through another PDMS casting process to add 2 mm thickness to the walls of the channel. Using this method, the channel's walls are thick enough to prevent them from deformation during the experiments. In addition, the inductor is close enough to the inner surface of the channel. These channels are

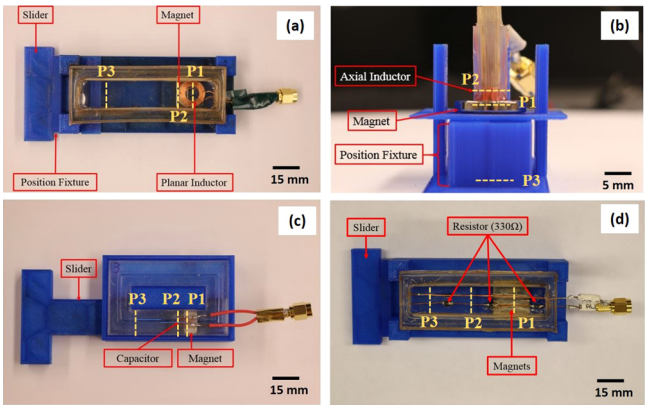

Figure 2. (a) Soft planar inductor placed on the 3D printed mount; a magnet installed on the slider can be stopped at the desired positions using the positioning fixture. (b) Axial inductor, (c) capacitor, and (d) resistor placed on the mount. P1, P2, and P3 indicate different positions of the mobile component during position-effect experiments.

40 mm long with a cross section of 3 mm × 3 mm. The process of fabricating axial inductors is illustrated in the Supporting Information (Figure S24).

The channel walls for the capacitors (Figure 2c) are made with PDMS using soft lithography technique and then attached to glass slides. Designing for a parallel plate capacitor, two slot gaps of 10 mm × 7 mm are considered on each side of the channel with 2.5 mm distance between them. These channels are 1.5 mm wide, 5 mm deep, and 152 mm long (the total loop length).

4.1.2. Electrical Components. The electrical components used in each unit are made of copper wires and copper plates. Although one can use liquid metals instead of copper to achieve more flexible and stretchable components, that is beyond the scope of this study.

For fabricating the planar inductor units, Mouser Electronics wireless charging coils WE-WPCC are used. We removed 10 rounds of wire from these coils to bring the SRF of the inductor (the frequency at which the parasitic capacitance of an inductor resonates with its inductance) to VNA's frequency range. These coils are attached to the bottom of the glass slides.

For the axial inductor units, copper wire of 28 gauge is wound around the channels over the length of 5 mm. The capacitor units are made of 10 mm × 7 mm copper plates embedded in the channel's slots. The resistor units are made of two parallel wires, each of which connects a series of resistors (Figure 2d). The conductive mobile component moves over both wires and connects them to make a closed circuit. Moving the mobile component back and forth on the wires changes the resistance as different number of resistors can be included in the circuit. A 26 gauge copper wire is used for connecting the series of resistors, and the second wire is 22 gauge. Three 330 Ω surface mounted device (SMD) resistors with 20 mm distance from each other are embedded in the unit. To obtain a continuous change in resistance, one can replace the copper wire and resistors with a high-resistance material.

4.1.3. Mobile Component. The mobile component is placed inside the channels and adds variability to each electrical unit. All the mobile components used in this study are magnetically responsive materials; thus, they can be controlled remotely while encapsulated in the channel. In

DOI: 10.1021/acsomega.9b02716
ACS Omega XXXX, XXX, XXX−XXX

Table 5. Levels of Iron Mass (g) and Ferrofluid Volume (μL) Used in Different Cases[a]

	iron (g)	magnet + iron (g)	magnet + ferrofluid (μL)	magnet + iron (g) + ferrofluid (μL)
planar (L1)	0.123 ± 0.006	0.027 ± 0.002	200	0.068 ± 0.015
planar (L2)	0.163 ± 0.019	0.049 ± 0.004	400	0.119 ± 0.019
planar (L3)[b]	**0.216 ± 0.013**	**0.109 ± 0.015**	**500**	**0.182 ± 0.066**
axial (L1)	0.102 ± 0.008	0.031 ± 0.006	20	0.033 ± 0.001
axial (L2)	0.136 ± 0.004	0.063 ± 0.005	30	0.065 ± 0.001
axial (L3)[b]	**0.171 ± 0.001**	**0.093 ± 0.012**	**40**	**0.096 ± 0.001**
capacitor (L1)	0.063 ± 0.003	0.127 ± 0.001	20	0.028 ± 0.002
capacitor (L2)	0.096 ± 0.003	0.155 ± 0.002	30	0.059 ± 0.001
capacitor (L3)[b]	**0.127 ± 0.001**	**0.186 ± 0.003**	**40**	**0.090 ± 0.002**
resistor (L1)	0.266 ± 0.001	0.116 ± 0.017	100	100
resistor (L2)	0.451 ± 0.001	0.234 ± 0.018	200	200
resistor (L3)[b]	**0.619 ± 0.001**	**0.447 ± 0.013**	**500**	**500**

[a]For magnet + iron + ferrofluid, iron mass is changed for inductors and capacitors and ferrofluid volume is changed for the resistors. The ferrofluid volume is 500 μL for the planar inductor and 40 μL for the axial inductor. In addition, the iron mass used for resistors under this case (magnet + iron + ferrofluid) is 0.447 ± 0.013 g. [b]Denotes the iron mass and ferrofluid volume used for position-effect studies.

this study, CMS Magnetics iron powder filings, Educational Innovation FF-310 bulk ferrofluid, and a mixture of both are used as the mobile component. To elaborate on the mixed mobile component, ferrofluid or iron powder (depending on the experiment) is simply combined while inside the channel. Ferrofluid is added using a pipette and the iron powder with a funnel. Further discussion of the mobile component can be found in the following sections and in Table 5. Permanent magnets are used as part of the actuation mechanism of the mobile component inside the channels.

Besides moving the mobile component in the channel, the magnet retains it in place after achieving the desired position. The choice of magnets and their configurations depend on the unit under study (Figure 3). For axial inductors, an axially

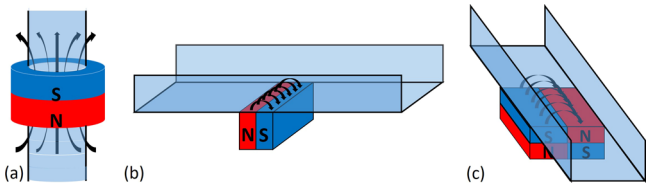

Figure 3. Configuration of magnets for each unit with respect to the channels. (a) Axial magnetized ring magnet surrounding a channel is used for axial inductors. (b) For planar inductors and capacitors, a single block magnet is placed such that both poles touch the channel. (c) Two magnet blocks attached to each other are used for the resistors.

magnetized ring magnet of NdFeB, Grade N42 with the outer diameter of 19 mm, the inner diameter of 9.5 mm, and thickness of 3.2 mm is used. This magnet slides up and down the inductor to achieve different positions for the mobile component. A block magnet of NdFeB, Grade N42 with dimensions of 19 mm × 9.5 mm × 6.35 mm magnetized through its thickness is used for the planar inductors and capacitors. Two of the same block magnets are used for resistors. The configurations of these magnets with respect to the channels are shown in Figure 3. A 3D printed position fixture is used for consistent positioning of magnets (Figure 2).

4.2. Experiments. Experiments are conducted in two different categories to explore the effect of position and quantity of the mobile component on the characteristics of the electrical units. In particular, inductance, capacitance, resistance, *Q*-factor, and SRF of the units are measured for different positions and quantities of the mobile component.

4.2.1. Quantity Effect. For the quantity-effect study, the amount of iron particles and ferrofluid volume are varied. For these measurements, the mobile component is placed at the center of the planar inductors, inside the axial inductors, between the plates for the capacitors, or between the first and the second SMD resistors. The four cases for this study are changing the mass of iron without the magnet being present (case (1)), changing the mass of iron with the magnet being present (case (2)), changing the mass of iron with the magnet and ferrofluid being present (case (3)), and changing the volume of ferrofluid with the magnet being present (case (4)). The amount of ferrofluid and iron used in these experiments are listed in Table 5.

4.2.2. Position Effect. For the position-effect study, the mobile component is moved to three different positions. These positions for each of the units are as follows. For planar inductor units, the mobile component is moved to (1) the center of the electrical component (P1), (2) its edge (P2), and (3) 50 mm from the center of it (P3). For axial inductor units, it is moved to (1) inside the electrical component (P1), (2) its edge (P2), and (3) 15 mm from the center of it (P3). For capacitor units, the mobile component is moved to (1) between the plates of the electrical component (P1), (2) its edge (P2), and (3) 30 mm from the center of those (P3). For resistor units, the three different positions of the mobile component correspond to having one (P1), two (P2), or three (P3) SMD resistors in the circuit. These positions are shown in Figure 2.

The iron mass and ferrofluid volume used for position-effect studies are highlighted in Table 5. The five different cases explored for this study include moving iron without the magnet being present (case (5)), iron with the magnet being present (case (6)), a mixture of iron and ferrofluid with the magnet being present (case (7)), ferrofluid with the magnet being present (case (8)), and only the magnet (case (9)).

4.3. Measurements. Measurements are conducted using an Agilent 8712ES VNA (Figure S2 in Supporting Information). The frequency range is kept the same for all three samples of each electronic unit but different between units. The scattering parameter indicating the reflection coefficient on port 1, S_{11}, is measured using one port measurement. The effect of cables and connections are

DOI: 10.1021/acsomega.9b02716
ACS Omega XXXX, XXX, XXX−XXX

carefully de-embedded using the built-in feature of the instrument and by separate measurements. The intermediate frequency bandwidth for all measurements is set to 250 Hz.

4.4. Calculations. Using the S_{11} parameter, the impedance parameter, Z, can be calculated using eq 1.

$$Z = Z_0\left(\frac{1 + S_{11}}{1 - S_{11}}\right) \quad (1)$$

where Z_0 is the characteristic impedance of VNA on port 1 (50 Ω in this case).

After obtaining Z-parameters over the frequency (f) range, inductance (L), capacitance (C), and Q-factor for each (Q_L and Q_C, respectively) can be expressed using eqs 2−5, respectively.

$$L = \frac{X_L}{\omega} = \frac{X_L}{2\pi f} \quad (2)$$

$$Q_L = \frac{\omega L}{r} = \frac{2\pi f L}{r} \quad (3)$$

$$C = \frac{1}{\omega X_C} = \frac{1}{2\pi f X_C} \quad (4)$$

$$Q_C = \frac{1}{\omega r C} = \frac{1}{2\pi f r C} \quad (5)$$

where X_L and X_C are the reactances (imaginary part of the Z-parameters) of the inductor and the capacitor, respectively. r is the equivalent series resistance of the component and ω is the resonance frequency.[47]

■ ASSOCIATED CONTENT

Supporting Information

The Supporting Information is available free of charge at https://pubs.acs.org/doi/10.1021/acsomega.9b02716.

Fabrication process of the axial inductors; image of a variable planar inductor connected to the VNA during the experiment; the effect of mobile component quantity and position on inductance, capacitance, or resistance, and Q-factor of the three planar inductor units, three axial inductor units, three capacitor units, and three resistor units plotted versus frequency; the spectral magnitude and spectral phase of the effect of mobile component quantity (a−d) and position (e−i) on inductance or capacitance and Q-factor of the three planar inductor units, three axial inductor units, and three capacitor units plotted versus frequency; experiments with the most significant change in the tuning range (a replication of Figure 1 in the semilog scale for the horizontal axis); mean, standard error of the mean (SEM), and the ratio of SEM/mean of a planar inductor's characteristics, an axial inductor's characteristics, a capacitor's characteristics, and a resistor's characteristics between three measurements at each position, tabulated; mean, SEM, and the ratio of SEM/mean of the percentage change in characteristics of planar inductors, axial inductors, capacitors, and resistors between three different samples of each type, tabulated; the correlations between the resulting inductance, capacitance, or impedance of planar and axial inductors, capacitors, and resistors and the position of the mobile component; the correlations between the resulting inductance, capacitance, or impedance of planar and axial inductors, capacitors, and resistors and the concentration of iron particles (PDF)

■ AUTHOR INFORMATION

Corresponding Author

*E-mail: hmarvi@asu.edu. Phone: 480-727-4853.

Funding

This work was funded through the start-up funding provided by Arizona State University.

Notes

The authors declare no competing financial interest.

The photographs in Figures 2 and S2 were taken by the authors.

■ ACKNOWLEDGMENTS

The authors would like to thank Kyle Xue for assistance with data collection. We also thank Arizona State University for funding this work.

■ REFERENCES

(1) Pang, C.; Lee, C.; Suh, K.-Y. Recent advances in flexible sensors for wearable and implantable devices. *J. Appl. Polym. Sci.* **2013**, *130*, 1429−1441.

(2) Majidi, C. Soft Matter Engineering for Soft Robotics. *Adv. Mater. Technol.* **2019**, *4*, 1800477.

(3) Yao, S.; Swetha, P.; Zhu, Y. Nanomaterial-Enabled Wearable Sensors for Healthcare. *Adv. Healthcare Mater.* **2018**, *7*, 1700889.

(4) Liu, Y.; Pharr, M.; Salvatore, G. A. Lab-on-Skin: A Review of Flexible and Stretchable Electronics for Wearable Health Monitoring. *ACS Nano* **2017**, *11*, 9614−9635.

(5) Wolfle, W. H.; Hurley, W. G. Quasi-active power factor correction with a variable inductive filter: theory, design and practice. *IEEE Trans. Power Electron.* **2003**, *18*, 248−255.

(6) James, J.; Boys, J.; Covic, G. A variable inductor based tuning method for ICPT pickups. *2005 International Power Engineering Conference*, 2005; Vol. 2, pp 1142−1146.

(7) Ito, Y.; Yoshihara, Y.; Sugawara, H.; Okada, K.; Masu, K. A 1.3-2.8 GHz Wide Range CMOS LC-VCO Using Variable Inductor. *2005 IEEE Asian Solid-State Circuits Conference*, 2005; pp 265−268.

(8) Zou, J.; Liu, C.; Schutt-Aine, J.; Chen, J.; Kang, S.-M. Development of a wide tuning range MEMS tunable capacitor for wireless communication systems. *International Electron Devices Meeting 2000. Technical Digest. IEDM (Cat. No.00CH37138)*, 2000; pp 403−406.

(9) Buyantuev, B.; Vorobev, E.; Turgaliev, V.; Kholodnyak, D.; Baskakova, A. Electrically controlled variable inductors for applications in tunable filters. *2018 22nd International Microwave and Radar Conference (MIKON)*, 2018; pp 487−491.

(10) Borwick, R. L.; Stupar, P. A.; DeNatale, J. F.; Anderson, R.; Erlandson, R. Variable MEMS capacitors implemented into RF filter systems. *IEEE Trans. Microw. Theory Tech.* **2003**, *51*, 315−319.

(11) Wang, C.; Wang, C.; Huang, Z.; Xu, S. Materials and Structures toward Soft Electronics. *Adv. Mater.* **2018**, *30*, 1801368.

(12) Yao, S.; Zhu, Y. Nanomaterial-enabled stretchable conductors: strategies, materials and devices. *Adv. Mater.* **2015**, *27*, 1480−1511.

(13) Trung, T. Q.; Lee, N. E. Recent Progress on Stretchable Electronic Devices with Intrinsically Stretchable Components. *Adv. Mater.* **2017**, *29*, 1603167.

(14) Park, S.; Mondal, K.; Treadway, R. M., III; Kumar, V.; Ma, S.; Holbery, J. D.; Dickey, M. D. Silicones for Stretchable and Durable Soft Devices: Beyond Sylgard-184. *ACS Appl. Mater. Interfaces* **2018**, *10*, 11261−11268.

(15) Oh, J. Y.; Lee, D.; Hong, S. H. Ice-Templated Bimodal-Porous Silver Nanowire/PDMS Nanocomposites for Stretchable Conductor. *ACS Appl. Mater. Interfaces* **2018**, *10*, 21666−21671.

DOI: 10.1021/acsomega.9b02716
ACS Omega XXXX, XXX, XXX−XXX

(16) Wagner, S.; Bauer, S. Materials for stretchable electronics. *MRS Bull.* **2012**, *37*, 207−213.
(17) Kim, D.-H.; Xiao, J.; Song, J.; Huang, Y.; Rogers, J. A. Stretchable, Curvilinear Electronics Based on Inorganic Materials. *Adv. Mater.* **2010**, *22*, 2108−2124.
(18) Rogers, J. A.; Someya, T.; Huang, Y. Materials and Mechanics for Stretchable Electronics. *Science* **2010**, *327*, 1603−1607.
(19) Choi, W. M.; Song, J.; Khang, D.-Y.; Jiang, H.; Huang, Y. Y.; Rogers, J. A. Biaxially stretchable wavy silicon nanomembranes. *Nano Lett.* **2007**, *7*, 1655−1663.
(20) Khang, D.-Y.; Jiang, H.; Huang, Y.; Rogers, J. A. A stretchable form of single-crystal silicon for high-performance electronics on rubber substrates. *Science* **2006**, *311*, 208−212.
(21) Kim, D.-H.; Song, J.; Choi, W. M.; Kim, H.-S.; Kim, R.-H.; Liu, Z.; Huang, Y. Y.; Hwang, K.-C.; Zhang, Y.-w.; Rogers, J. A. Materials and noncoplanar mesh designs for integrated circuits with linear elastic responses to extreme mechanical deformations. *Proc. Natl. Acad. Sci. U.S.A.* **2008**, *105*, 18675−18680.
(22) Hsu, Y.-Y.; Gonzalez, M.; Bossuyt, F.; Vanfleteren, J.; De Wolf, I. Polyimide-enhanced stretchable interconnects: design, fabrication, and characterization. *IEEE Trans. Electron Devices* **2011**, *58*, 2680−2688.
(23) Rosset, S.; Niklaus, M.; Dubois, P.; Shea, H. R. Metal ion implantation for the fabrication of stretchable electrodes on elastomers. *Adv. Funct. Mater.* **2009**, *19*, 470−478.
(24) Kaltenbrunner, M.; Kettlgruber, G.; Siket, C.; Schwödiauer, R.; Bauer, S. Arrays of ultracompliant electrochemical dry gel cells for stretchable electronics. *Adv. Mater.* **2010**, *22*, 2065−2067.
(25) Lanzara, G.; Salowitz, N.; Guo, Z.; Chang, F.-K. A Spider-Web-Like Highly Expandable Sensor Network for Multifunctional Materials. *Adv. Mater.* **2010**, *22*, 4643−4648.
(26) Lewis, J. S.; Weaver, M. S. Thin-film permeation-barrier technology for flexible organic light-emitting devices. *IEEE J. Sel. Top. Quantum Electron.* **2004**, *10*, 45−57.
(27) Gray, D. S.; Tien, J.; Chen, C. S. High-Conductivity Elastomeric Electronics. *Adv. Mater.* **2004**, *16*, 393−397.
(28) Dickey, M. D. Emerging applications of liquid metals featuring surface oxides. *ACS Appl. Mater. Interfaces* **2014**, *6*, 18369−18379.
(29) Lu, T.; Wissman, J.; Ruthika, C.; Majidi, C. Soft anisotropic conductors as electric vias for ga-based liquid metal circuits. *ACS Appl. Mater. Interfaces* **2015**, *7*, 26923−26929.
(30) Jeon, J.; Lee, J.-B.; Chung, S. K.; Kim, D. On-demand magnetic manipulation of liquid metal in microfluidic channels for electrical switching applications. *Lab Chip* **2017**, *17*, 128−133.
(31) Wang, M.; Trlica, C.; Khan, M. R.; Dickey, M. D.; Adams, J. J. A reconfigurable liquid metal antenna driven by electrochemically controlled capillarity. *J. Appl. Phys.* **2015**, *117*, 194901.
(32) Pamme, N. Magnetism and microfluidics. *Lab Chip* **2006**, *6*, 24−38.
(33) Love, L. J.; Jansen, J. F.; McKnight, T. E.; Roh, Y.; Phelps, T. J.; Yeary, L. W.; Cunningham, G. T. Ferrofluid field induced flow for microfluidic applications. *IEEE ASME Trans. Mechatron.* **2005**, *10*, 68−76.
(34) Zeng, J.; Deng, Y.; Vedantam, P.; Tzeng, T.-R.; Xuan, X. Magnetic separation of particles and cells in ferrofluid flow through a straight microchannel using two offset magnets. *J. Magn. Magn. Mater.* **2013**, *346*, 118−123.
(35) Hartshorne, H.; Backhouse, C. J.; Lee, W. E. Ferrofluid-based microchip pump and valve. *Sens. Actuators, B* **2004**, *99*, 592−600.
(36) Oh, D.-W.; Jin, J. S.; Choi, J. H.; Kim, H.-Y.; Lee, J. S. A microfluidic chaotic mixer using ferrofluid. *J. Micromech. Microeng.* **2007**, *17*, 2077.
(37) Tan, S.-H.; Nguyen, N.-T.; Yobas, L.; Kang, T. G. Formation and manipulation of ferrofluid droplets at a microfluidicT-junction. *J. Micromech. Microeng.* **2010**, *20*, 045004.
(38) Borduz, L.; Raj, K. Low viscosity, electrically conductive ferrofluid composition and method of making and using same. U.S. Patent 4,687,596A, 1987.
(39) Mehta, R. V.; Upadhyay, R. V.; Dasannacharya, B. A.; Goyal, P. S.; Rao, K. S. Magnetic properties of laboratory synthesized magnetic fluid and their temperature dependence. *J. Magn. Magn. Mater.* **1994**, *132*, 153−158.
(40) Pant, R.; Dhawan, S.; Suri, D.; Arora, M.; Gupta, S.; Koneracká, M.; Kopčanský, P.; Timko, M. Synthesis and characterization of ferrofluid-conducting polymer composite. *Indian J. Eng. Mater. Sci.* **2004**, *11*, 267−270.
(41) Carle, F.; Bai, K.; Casara, J.; Vanderlick, K.; Brown, E. Development of magnetic liquid metal suspensions for magneto-hydrodynamics. *Phys. Rev. Fluids* **2017**, *2*, 013301.
(42) Lazarus, N.; Meyer, C. D.; Bedair, S. S.; Nochetto, H.; Kierzewski, I. M. Multilayer liquid metal stretchable inductors. *Smart Mater. Struct.* **2014**, *23*, 085036.
(43) Assadsangabi, B.; Ali, M. M.; Takahata, K. Ferrofluid-based variable inductor. *Micro Electro Mechanical Systems (MEMS), 2012 IEEE 25th International Conference*, 2012; pp 1121−1124.
(44) Polcar, P.; Mayer, D. Magnetic Field Controlled Capacitor. *J. Electr. Eng.* **2016**, *67*, 227.
(45) Liu, S.; Sun, X.; Hildreth, O. J.; Rykaczewski, K. Design and characterization of a single channel two-liquid capacitor and its application to hyperelastic strain sensing. *Lab Chip* **2015**, *15*, 1376−1384.
(46) Xia, Y.; Whitesides, G. M. Soft lithography. *Angew. Chem., Int. Ed.* **1998**, *37*, 550−575.
(47) Hiscocks, P. *Analog Electronic Circuit Design*; John Wiley & Sons, Inc., 2006.

DOI: 10.1021/acsomega.9b02716
ACS Omega XXXX, XXX, XXX−XXX